

# Electrochemical and microscopic characterisation of platinum-coated perfluorosulfonic acid (Nafion 117) materials†



Sally-Ann Sheppard,<sup>a†</sup> Sheelagh A. Campbell,<sup>a</sup> James R. Smith,<sup>a</sup> Grongar W. Lloyd,<sup>a‡</sup> Thomas R. Ralph<sup>b</sup> and Frank C. Walsh<sup>a\*</sup>

<sup>a</sup> Applied Electrochemistry Group and Scanning Probe Microscopy Laboratory, School of Pharmacy and Biomedical Sciences, University of Portsmouth, St. Michael's Building, White Swan Road, Portsmouth, UK PO1 2DT

<sup>b</sup> Johnson Matthey Technology Centre, Blount's Court, Sonning Common, Reading, UK RG4 9NH

Received 1st April 1998, Accepted 28th July 1998

Platinum-coated Nafion 117 structures were characterised using electrochemical measurements of platinum surface area and a number of microscopy techniques. The morphology and composition of the platinum deposits were related to their preparation conditions in terms of platinum salt concentration, electrolyte flow and the surface roughness of Nafion 117. Platinum surface areas achieved were higher than the values predicted for ideal spherical platinum particles of average diameter. This is due to a fine microstructure, which realises much smaller platinum particles than average (down to about 50 nm) allied to the geometry produced by their clustering to form nodules (about 0.1–1.5 µm diameter micro-nodules and about 3–5 µm macro-nodules). Adherent platinum deposits with high surface areas were promoted by using roughened Nafion 117 membranes and enhancing the mass transport of chloroplatinate and tetraborohydrate ions by magnetic stirring of the electrolyte. A flow cell produced much more reproducible platinum-coated Nafion 117 structures. At best, platinum surface areas of 30–50 m<sup>2</sup> g<sup>-1</sup> Pt were achieved at platinum penetration depths of 5–30 µm into the membrane surface.

## Introduction

Fluorocarbon ion-exchange membranes coated or laminated to an electrocatalyst layer have become essential components in many electrochemical devices, including proton exchange membrane fuel cells,<sup>1</sup> electrolysis cells<sup>2</sup> and more recently a wide range of sensor devices. For example, an amperometric flow cell incorporating a Pt/Nafion sensor electrode has been successfully used for the amperometric determination of quinones, amines and phenols in aqueous solution and also for hydrazine, hydroquinone, oxalic acid, ascorbic acid and tetra-cyanoquinodimethane (TCNQ).<sup>3</sup>

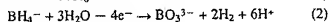
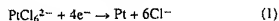
DuPont first developed perfluorinated membranes in the early 1960s under the trade-name Nafion. These ion-exchange membranes<sup>4</sup> are copolymers of tetrafluoroethylene and perfluorinated vinyl ethers containing terminal sulfonyl fluoride groups. Such terminal groups are then treated to produce the proton conducting –SO<sub>3</sub>H (or –CO<sub>2</sub>H) groups. The ionic structure and properties of ionomers such as Nafion have been discussed in detail elsewhere.<sup>4–11</sup> Nafion is frequently used in fuel cell and electrolysis applications as a result of an excellent chemical and mechanical stability allied to a high ionic conductivity.<sup>12</sup>

Nafion ion-exchange materials produce highly acidic environments as a consequence of the sulfonic acid groups located within the micelle structure.<sup>7</sup> Thus noble metals (most notably platinum) or their oxides are often the electrocatalysts of choice for coating or laminating to the solid polymer electrolyte (SPE).<sup>13</sup> Since noble metal coated SPEs are high cost materials,

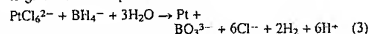
for the majority of applications low noble metal loadings are required to limit costs. Further, at such loadings, it is important to maximise the active metal surface area to achieve a high metal dispersion on the SPE to promote the desired reaction(s). Good adhesion of the electrocatalyst to the membrane is also necessary to reduce ohmic losses and to support the high mechanical stresses produced during operation. Such stresses arise due to dimensional changes in the membrane during hydration, dehydration and gas evolution, which often accompany the main reaction(s) in electrosynthesis applications.

There are several methods of depositing metal coatings on membrane surfaces, notably mechanically pressing<sup>14</sup> electrochemical deposition<sup>15,16</sup> and chemical deposition.<sup>17,18</sup> In this study, a chemical reduction route, first reported by Takenaka and co-workers,<sup>17,18</sup> was used to deposit platinum on one side of a Nafion 117 membrane.

In this method, solutions of platinum anions, such as chloroplatinate (PtCl<sub>6</sub><sup>2-</sup>), and a reducing agent, typically tetrahydroborate ion (BH<sub>4</sub><sup>-</sup>), are exposed to opposite sides of a stationary SPE membrane. BH<sub>4</sub><sup>-</sup> ions continuously penetrate the membrane and come into contact with PtCl<sub>6</sub><sup>2-</sup> ions on the opposite membrane face, at which point the platinum ions are reduced to platinum metal at the membrane surface according to the redox reactions:



to give the overall process:



Here, cyclic voltammetry,<sup>19</sup> atomic force microscopy (AFM),<sup>20</sup> scanning electron microscopy (SEM), transmission electron microscopy (TEM) and electron probe microanalysis (EPMA)<sup>21</sup> were used to characterise platinum-coated Nafion 117 membranes under a variety of synthesis conditions.

† Presented at EIRELEC '98, Howth, Co. Dublin, Ireland, March 26–28, 1998.

‡ Present address: INCO Europe Ltd., Acton Refinery, North Acton, London, UK NW10 6SN.

\* Present address: GL Instruments, 5 Chichester Walk, Banbury, Oxford, UK OX16 7YT.

## Experimental

The Nafion 117 membrane (nominal thickness 178  $\mu\text{m}$ , Sigma-Aldrich, Dorset, UK) was boiled in de-ionised water for 2 h prior to platinum deposition. A circular disc of the protonated form of Nafion 117 (6.25  $\text{cm}^2$ ) was mounted vertically between polypropylene flanges closed at one end to accommodate electrolyte. One membrane face was exposed to 25  $\text{cm}^3$  of  $\text{H}_2\text{PtCl}_6$  (AR grade, Fisher Scientific UK, Loughborough, UK) and the opposite face was simultaneously exposed to 90  $\text{cm}^3$  of 0.1  $\text{mol dm}^{-3}$   $\text{NaBH}_4$  (SLR grade, Fisher Scientific UK) in 1  $\text{mol dm}^{-3}$   $\text{NaOH}$  (SLR grade, Fisher Scientific UK). The reaction time was typically limited to 3 h at 295 K. Surface roughening of Nafion 117 was achieved by abrasion with 1200 grade silicon carbide paper prior to placing it in the deposition cell. The deposition process created large amounts of hydrogen [reaction (3)] which needed to be removed to minimise the effect on the platinum deposition. This was achieved by agitating the electrolyte either through manual shaking of the cell at regular (10–15 min) intervals, by magnetically stirring the electrolyte or by placing the cell in a mechanical shaker. Prior to electrochemical studies, the Pt/Nafion samples were soaked for approximately 16 h in 1  $\text{mol dm}^{-3}$   $\text{H}_2\text{SO}_4$  (AR grade, Fisher Scientific UK) at 295 K to leave the membrane in a hydrated, acid form.

In a modified procedure, hydrogen was removed in a controlled manner using a flow-through cell (Fig. 1). The cell was machined from four blocks of polypropylene (each 3 cm wide  $\times$  5 cm long  $\times$  1 cm thick). The inner polypropylene blocks formed the electrolyte channels. The  $\text{H}_2\text{PtCl}_6$  and  $\text{NaBH}_4$  flow channels were separated by the Nafion 117 membrane, exposing a membrane surface area of 2.35  $\text{cm}^2$ . Silicone rubber gaskets were placed between each of the four blocks to prevent leakage. The cell was held together with six brass tie-rods. The  $\text{H}_2\text{PtCl}_6$  and  $\text{NaBH}_4$  reservoirs were filled with 80  $\text{cm}^3$  of solution at a temperature of approximately 295 K. The reactant solutions were circulated using two Totton EMP 50/7 pumps. The flow was measured volumetrically before and after each experiment.

The platinum loading on the Pt/Nafion electrodes was determined by the mass difference of the Nafion membrane before and after metal deposition. The membranes were boiled in de-ionised water for 1 h prior to deposition and dried for 20–24 h at 353 K and 740 mmHg to constant mass both before and after deposition.

The real surface area of a catalyst can be orders of magnitude greater than the geometric area. Since adsorption and catalytic reaction rates are based on real surface area, it is important to be able to measure this value. An accepted electrochemical method

of estimating the surface area of platinum is to measure the saturated hydrogen coverage,  $\theta_{\text{H}}$ , of the platinum from a cyclic voltammogram after subtracting the double layer charge. Fig. 2 shows a cyclic voltammogram of a Pt/Nafion surface obtained after 10 h of potential cycling between the limits 0 and 1.5 V versus SHE at a potential sweep rate of 40  $\text{mV s}^{-1}$  in 1  $\text{mol dm}^{-3}$   $\text{H}_2\text{SO}_4$  at 295 K. The established features of hydrogen adsorption, hydrogen desorption, double layer charging, oxide formation and oxide reduction are evident as peaks in the voltammogram.<sup>19</sup> It is assumed that each surface platinum atom is associated with one chemisorbed hydrogen atom, allowing the charge corresponding to the area under the strong and weak hydrogen adsorption peaks,  $Q_{\text{H}}$ , to be converted to the real electrochemical surface area. When polycrystalline surfaces are considered, the conversion of the adsorption charge to the real surface area is 210  $\mu\text{C cm}^{-2}$  Pt. This value has been generally accepted as a conversion standard.<sup>19</sup>

$$A_{\text{ec}} = Q_{\text{H}}/Q_{\text{m}} \quad (4)$$

where  $A_{\text{ec}}$  is the real electrochemical surface area ( $\text{cm}^2$  Pt),  $Q_{\text{H}}$  is the saturated hydrogen coverage on the electrode ( $\mu\text{C}$ ) and  $Q_{\text{m}}$  is the electrical charge associated with monolayer adsorption of hydrogen ( $Q_{\text{m}} = 210 \mu\text{C cm}^{-2}$  Pt).

The enhancement of real electrochemical surface area, in comparison with a smooth surface, can be described by a roughness factor ( $\text{cm}^2$  Pt  $\text{cm}^{-2}$ ):

$$R_{\text{F}} = A_{\text{ec}}/A_{\text{g}} \quad (5)$$

where  $A_{\text{ec}}$  is the real electrochemical surface area ( $\text{cm}^2$  Pt) and  $A_{\text{g}}$  is the geometric surface area ( $\text{cm}^2$ ), which is a circular disc in the present work.

AFM studies were performed in air under normal atmospheric conditions using a Discoverer TopoMetric TMX2000 scanning probe microscope (SPM) (TopoMetric, Safran Walden, Essex, UK). Samples were mounted on a conductive carbon support and imaged uncoated. A scanner capable of a maximum x,y,z-translation of  $75 \times 75 \times 12 \mu\text{m}$  was used and imaging was performed in contact mode using forces in the range of 1–10 nN. Imaging was restricted to platinum deposits with a surface relief of less than 16  $\mu\text{m}$  owing to limitations in the z-range of the scanners piezo-element. Standard profile, silicon nitride tips, mounted on cantilevers of spring constant 0.036  $\text{N m}^{-1}$ , were used and the graphic output was displayed on a monitor with a resolution of 400 lines by 400 pixels. Images were levelled by plane fitting and shaded to enhance topographic features; quantitative data were extracted from levelled images.

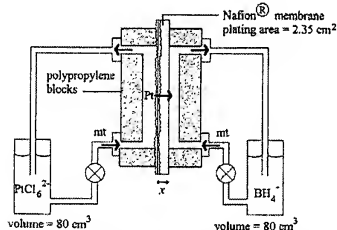


Fig. 1 Schematic diagram of the flow-through cell used to deposit Pt on a Nafion 117 membrane via a diffusion process through the membrane involving tetrahydroborate ion reduction of chloroplatinic ions,  $x = \text{Pt}$  deposit nominal thickness (178  $\mu\text{m}$ ); mt = mass transport of species.

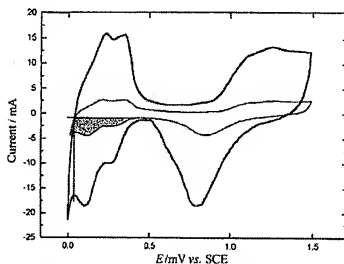


Fig. 2 Cyclic voltammograms of Pt-coated Nafion 117 membrane in 1  $\text{mol dm}^{-3}$   $\text{H}_2\text{SO}_4$  at 295 K. The inner voltammogram (thin line) was obtained for a low platinum loading (1.2  $\text{mg Pt cm}^{-2}$ ) and the outer (bold line) for a higher platinum loading (6.4  $\text{mg Pt cm}^{-2}$ ). The shaded regions on the voltammograms represent the hydrogen adsorption charge,  $Q_{\text{H}}$ , used in the surface area measurement. Potential sweep rate: 40  $\text{mV s}^{-1}$ .

EPMA was performed using a Camcbar SX500 instrument. A section of the Pt/Nafion sample was mounted in resin (Struers Epafix) reinforced with alumina particles. The surface was polished using silicon carbide papers then diamond paste down to a surface roughness of less than 0.1  $\mu\text{m}$ . It was vacuum coated with an approximately 20 nm thickness of carbon to provide an electrically conductive surface. The sample was examined using a beam current of 20 nA and an accelerating voltage of 20 kV. For each Pt/Nafion sample, a peak and background pair of line scans was obtained across the platinum deposit and into the membrane. For the uncoated membrane, a peak and background pair of line scans was run across a portion of the surface. The background signals were subtracted from the peak signals to produce peak-background corrected line scans for platinum and fluorine.

SEM was performed on a Licca Electron Optics S250 instrument using an accelerating voltage of 20 kV. The Pt/Nafion samples were mounted on a specimen grid and cooled in liquid nitrogen to 77 K and cut with a blade to examine cross-sections. Secondary and backscattered electron micrographs were obtained. TEM utilised a Philips EM400T electron microscope using an acceleration voltage of 100 kV with bright and dark-field illumination. The Pt/Nafion samples were supported on carbon-coated grids.

## Results and discussion

### Effect of chloroplatinic acid concentration on platinum deposition

The mass of platinum deposited and the platinum surface area were mainly affected by the reactant concentration, the flux of the diffusing reactants, the deposition time and the temperature. In the first experiments, the  $\text{H}_2\text{PtCl}_6$  concentration was treated as a major variable. The other variables were kept constant, with manual shaking of the cell initially used to remove hydrogen gas bubbles produced during the deposition process [reaction (3)].

Fig. 3(a) shows the effect of  $\text{H}_2\text{PtCl}_6$  concentration on the mass of platinum deposited. This increased with  $\text{H}_2\text{PtCl}_6$  concentration, although the relationship was non-linear with the platinum loading increasing only slightly at higher  $\text{H}_2\text{PtCl}_6$  levels. The roughness factor, which is the ratio of real electrochemical surface area to geometric area, also increased with  $\text{H}_2\text{PtCl}_6$  in a non-linear fashion, as shown in Fig. 3(b).

In Fig. 3(c), the results from Fig. 3(a) and (b) are correlated in the form of a roughness factor *versus* platinum-loading plot. Again, a non-linear relationship is evident and there is a relatively large region between 1.2 and 3.5  $\text{mg Pt cm}^{-2}$  where the roughness factor increases only slightly with increase in platinum loading. At a platinum loading higher than approximately 3.5  $\text{mg Pt cm}^{-2}$ , the roughness factor increases much more steeply. There is a clear trade-off between obtaining high  $R_F$  values corresponding to high real electrochemical surface areas and the production of high loading to give thick, expensive platinum deposits.

It is useful to rationalise the experimental roughness factors obtained from hydrogen adsorption coulometry by comparing the data with the predictions of a simple model.<sup>12</sup> The platinum deposit can be naively considered as a homogeneous distribution of smooth, non-porous, spherical particles, each of diameter  $d$  (cm). The specific surface area,  $S$  ( $\text{cm}^2 \text{g}^{-1} \text{Pt}$ ), is then given by

$$S = 6/\rho d \quad (6)$$

where  $\rho$  is the density of platinum ( $21.41 \text{ g cm}^{-3}$ ). The specific surface area may also be related to the real and geometric values of area ( $A_r$  and  $A_g$ ) and the platinum loading,  $W$  ( $\text{g Pt cm}^{-2}$ ), by

$$S = (A_r/A_g)(1/W) \quad (7)$$

Since in this study  $A_{\text{ex}}$  is used to measure  $A_r$ , the roughness factor can be described as

$$R_F = SW \quad (8)$$

The selection of an appropriate value for  $d$  is difficult, as microscopy shows that a wide distribution of platinum particle sizes exists. For the purposes of calculation, 100 nm may be taken as an average particle diameter measured in SEM, AFM and TEM images. Application of eqn. (6) to calculate  $S$  and eqn. (8) to give the theoretical  $R_F$  *versus*  $W$  relationship produces the dotted straight line shown in Fig. 3(c). The experimental data provide roughness factors that are considerably higher than the predicted values. This is illustrated by the model predictions shown by the dashed lines in Fig. 3(c), which indicate that a much better fit is obtained for platinum particle diameters below 50 nm. The simple model cannot, however, accommodate the rapid rise in  $R_F$  at high platinum loadings, which corresponds to an increase in the specific surface area of the deposit.

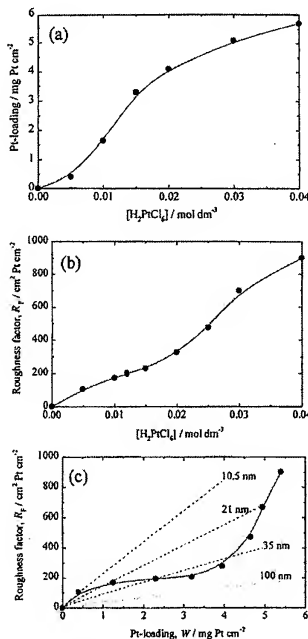


Fig. 3 Relationship between chloroplatinic acid concentration, platinum loading and roughness factor. Deposition conditions: 0.1 mol dm<sup>-3</sup> NaBH<sub>4</sub> in 1 mol dm<sup>-3</sup> NaOH; 3 h deposition time;  $T = 295 \text{ K}$ ; Nafion 117 surface not roughened prior to platinising; manual shaking employed. (a) Dependence of platinum-loading on chloroplatinic acid concentration; (b) dependence of roughness factor on chloroplatinic acid concentration; (c) roughness factor as a function of platinum loading for the data in (a) and (b). The slope of the curve represents the specific surface area of the platinum deposit. The dotted line shows the predictions of a simple model, assuming deposition of smooth, non-porous, homogeneous, spherical particles of Pt having a diameter of 100 nm. The dashed lines show the model predictions for a range of Pt particle diameters.

Investigating the morphology of the platinum deposit highlighted the reason for the high  $R_F$  values. Fig. 4(a) shows a typical scanning electron micrograph of a high platinum loading membrane sample ( $6.4 \text{ mg Pt cm}^{-2}$ ) prepared using  $0.02 \text{ mol dm}^{-3} \text{ H}_2\text{PtCl}_6$  and  $0.1 \text{ mol dm}^{-3} \text{ NaBH}_4$  in  $1 \text{ mol dm}^{-3} \text{ NaOH}$  with a 3 h deposition time and manual shaking of the cell. A smooth, 'mud-cracked' surface is evident with macro-nodules  $2\text{--}4 \text{ mm}$  wide on islands of width  $40\text{--}100 \text{ }\mu\text{m}$  formed by the cracks in the deposit. The cracks are approximately  $1 \text{ }\mu\text{m}$  across and were shown to arise during the deposition process itself, rather than from subsequent drying effects. This cracking, which may be caused by an increase in the internal tensile stress in the deposit, may limit the lifetime of the electrode structure in some applications by allowing liquid electrolyte ingress, thereby undermining the deposit and perhaps promoting membrane degradation. Following cracking early in the deposition process, subsequent layers of platinum grew in the cracks, giving rise to a two-layered structure shown in Fig. 4(b). Backscattered electron imaging showed that the platinum had deposited relatively uniformly across the SPE surface, the nominal deposit thickness being approximately  $5 \text{ }\mu\text{m}$ .

At a lower platinum loading, the noble metal coating showed similar features. For example, SEM studies were also performed on a relatively low platinum loading surface ( $1.2 \text{ mg Pt cm}^{-2}$ ) prepared from  $0.01 \text{ mol dm}^{-3} \text{ H}_2\text{PtCl}_6$  and  $0.1 \text{ mol dm}^{-3} \text{ NaBH}_4$  in  $1 \text{ mol dm}^{-3} \text{ NaOH}$ , with a 3 h deposition time and manual shaking of the cell. As expected, a thin platinum coating was formed. In fact, backscattered electron imaging indicated the average deposit thickness was only  $0.2 \text{ }\mu\text{m}$  and an incomplete surface coverage of the Nafion membrane was obtained. In the plated regions, macro-nodules,  $1.0\text{--}2.5 \text{ }\mu\text{m}$

wide, were evident on islands of width  $100\text{--}180 \text{ }\mu\text{m}$  divided by cracks typically  $2\text{--}4 \text{ }\mu\text{m}$  across.

Closer examination of the relatively 'flat' regions of the surface of the Pt/Nafion structures (with a surface relief less than  $16 \text{ }\mu\text{m}$ ) using AFM provided further insight into the topography. A typical AFM micrograph of the Pt/Nafion membrane is shown in Fig. 5(a). As evidenced by SEM, the deposit can be considered as a series of macro-nodules typically  $0.7\text{--}3.2 \text{ }\mu\text{m}$  in diameter. In Fig. 5(a), AFM clearly shows, however, that these are made up from micro-nodule assemblies of diameter  $0.1\text{--}1.5 \text{ }\mu\text{m}$ . Most importantly, closer examination by TEM revealed a finer grain structure down to  $50 \text{ nm}$  diameter. Such findings are comparable to those in studies using an impregnation-reduction technique with a  $[\text{Pt}(\text{NH}_3)_4]^{2+}$  salt.<sup>12</sup> As shown in Fig. 3(c), smaller platinum particles give higher  $R_F$  values, but with the Pt/Nafion electrodes, since  $d \approx 100 \text{ nm}$ , it is the fine microstructure allied to the way in which the small ( $50\text{--}100 \text{ nm}$ ) platinum particles cluster to form complex 3D geometries that produces the high  $R_F$  values. Further, the rapid rise in  $R_F$  at high platinum loading is probably attributable to the effect of the macro-nodules, evident in Fig. 5(a). Certainly the macro-nodules are more likely to be formed at high platinum loading. They may alter the packing of the fine microstructure in a fashion that increases the specific surface area. This macro-nodule formation may be due to heterogeneity in the membrane structure allowing preferential deposition of platinum at specific membrane sites. Some indication of this is given by the difficulty in reproducing macro-nodule formation, with similar preparation conditions giving platinum deposits having varying numbers of macro-nodules.

In addition to the  $R_F$  versus  $W$  relationship, the adhesion of the deposit is very important. EPMA was used to investigate the location of the platinum. Three distinct regions were found, (i)

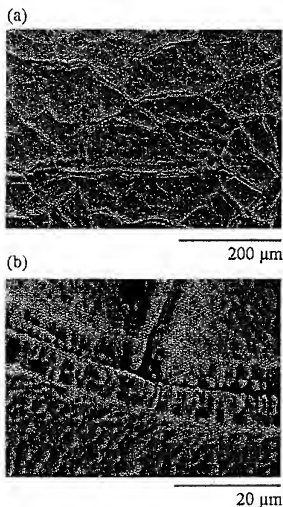


Fig. 4 Scanning electron micrograph of a Pt-coated Nafion 117 membrane surface containing a high platinum loading ( $6.4 \text{ mg Pt cm}^{-2}$ ). The deposit was obtained from  $0.02 \text{ mol dm}^{-3} \text{ H}_2\text{PtCl}_6$  and  $0.1 \text{ mol dm}^{-3} \text{ NaBH}_4$  in  $1 \text{ mol dm}^{-3} \text{ NaOH}$  which had been manually shaken during a deposition time of 3 h.  $T = 295 \text{ K}$  with the membrane surface not roughened prior to platinum deposition. Image (b) is an enlarged region of one of the cracked regions seen in image (a).

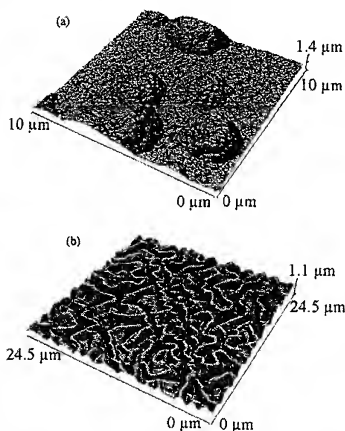


Fig. 5 Atomic force micrographs of Pt-coated Nafion 117 membrane prepared under two different deposition conditions: (a)  $0.03 \text{ mol dm}^{-3} \text{ H}_2\text{PtCl}_6$  and  $0.1 \text{ mol dm}^{-3} \text{ NaBH}_4$  in  $1 \text{ mol dm}^{-3} \text{ NaOH}$  manually shaken during a deposition time of 3 h.  $T = 295 \text{ K}$ , with membrane surface not roughened prior to platinum deposition. (b) structure obtained using a flow-through cell, using  $0.02 \text{ mol dm}^{-3} \text{ H}_2\text{PtCl}_6$  ( $v = 4.3 \text{ cm s}^{-1}$ ) and  $0.1 \text{ mol dm}^{-3} \text{ NaBH}_4$  in  $1 \text{ mol dm}^{-3} \text{ NaOH}$  ( $v = 4.3 \text{ cm s}^{-1}$ ) over a 4 h deposition time,  $T = 295 \text{ K}$ , with the membrane surface pre-roughened prior to platinum deposition.

an external platinum deposit, (ii) platinum inside the membrane and (iii) very low levels of isolated platinum particles deeper inside the membrane which cannot take part in any reaction. For example, background corrected line scans for platinum and fluorine for a typical Pt/Nafion membrane prepared using  $0.02 \text{ mol dm}^{-3} \text{ H}_2\text{PtCl}_6$  and  $0.1 \text{ mol dm}^{-3} \text{ NaBH}_4$  in  $1.0 \text{ mol dm}^{-3} \text{ NaOH}$  with manual shaking of the cell are shown in Fig. 6. The depth probed was approximately  $60 \mu\text{m}$  into the Nafion 117 material. It is clear that the fluorine level varies considerably in Nafion 117, reflecting the heterogeneous nature of fluorine distribution within the fluorinated polymer network. Fig. 6 shows, however, from the overlap of the platinum and fluorine line scans that platinum has penetrated to a depth of less than  $10 \mu\text{m}$  into the membrane. When the concentration of  $\text{H}_2\text{PtCl}_6$  was reduced from  $0.02$  to  $0.01 \text{ mol dm}^{-3}$ , the top  $5\text{--}10 \mu\text{m}$  region of the Pt/Nafion electrodes appeared to be particularly well enriched with platinum. This is in agreement with the findings of Kamasaki *et al.*,<sup>23</sup> who found that by increasing the  $\text{H}_2\text{PtCl}_6$  concentration, a more adherent deposit could be obtained. As the  $\text{H}_2\text{PtCl}_6$  concentration increases, more platinum is deposited inside the membrane and hence the adhesion is improved. With manual shaking of the cell, however, the depth of platinum penetration did not exceed  $10 \mu\text{m}$ .

### Effect of solution agitation

The electrolyte flow conditions are known to be important during the chemical deposition of platinum.<sup>19,20</sup> Solution agitation is necessary to remove hydrogen gas bubbles from the membrane surface, which interferes with platinum deposition and reduces the roughness factor and specific surface area. Improved agitation also controls adhesion of the precious metal to the membrane surface. The ionic transport of  $\text{PtCl}_6^{2-}$  and  $\text{BH}_4^-$  ions within the membrane, which is restricted by electrostatic repulsion of the sulfonic acid groups, is raised. This reduces the concentration polarisation effects within the membrane and extends the penetration depth at which reduction first occurs.<sup>23</sup>

Consequently, alternative methods of solution agitation were investigated. Table 1 summarises the effect of using four types of solution agitation on the platinum loading, roughness factor and specific surface area of the Nafion 117 structures. In these studies, the platinum loading was maintained at a relatively high level ( $3.9\text{--}5.5 \text{ mg Pt cm}^{-2}$ ) to provide a readily contacted conductive coating of platinum. Table 1 clearly shows that

manually shaking the deposition cell at regular intervals produced the lowest  $R_f$  value and platinum surface area ( $7.1 \text{ m}^2 \text{ g}^{-1} \text{ Pt}$ ). This suggests that the hydrogen formed during the reduction process was not efficiently removed from the membrane surface. This inhibited platinum nucleation, resulting in an increased platinum particle size and a lowering of the  $R_f$  value and platinum specific surface area. Magnetic stirring of the electrolyte gave a slightly higher deposition rate and an increased  $R_f$  value and platinum specific surface area ( $16.7 \text{ m}^2 \text{ g}^{-1} \text{ Pt}$ ). In this case, the hydrogen was removed more efficiently from the membrane surface, producing more platinum nucleation sites and, hence, a smaller platinum particle size and higher platinum surface area. EPMA also showed a greater degree of platinum penetration of the membrane at a given  $\text{H}_2\text{PtCl}_6$  concentration. Mechanically shaking the cell showed little increase in the platinum surface area, *i.e.*, even at  $5.5 \text{ mg Pt cm}^{-2}$  the specific surface area was only  $10.3 \text{ m}^2 \text{ g}^{-1} \text{ Pt}$ . EPMA also showed that at a similar  $\text{H}_2\text{PtCl}_6$  concentration the platinum was deposited much closer to the surface of the membrane compared with manual shaking of the cell. Mechanically shaking the cell did not provide an efficient method of preparing Pt/Nafion structures.

As a consequence of the success of magnetic stirring, a flow-through cell was designed and built (Fig. 1) to provide a reproducible mass transport regime by controlling the mean linear velocity of the electrolytes during the chemical reduction process.

Fig. 5(b) shows an atomic force micrograph of a platinum-coated Nafion structure ( $3.8 \text{ mg Pt cm}^{-2}$ ) obtained after 4 h using the flow-through cell with  $0.02 \text{ mol dm}^{-3} \text{ H}_2\text{PtCl}_6$  ( $v = 4.3 \text{ cm s}^{-1}$ ) and  $0.1 \text{ mol dm}^{-3} \text{ NaBH}_4$  in  $1 \text{ mol dm}^{-3} \text{ NaOH}$  ( $v = 4.3 \text{ cm s}^{-1}$ ). An extremely regular platinum deposit was obtained. The smooth ripple effect indicates the direction of the solution flow. Typical peak dimensions were  $1.5 \mu\text{m}$  in diameter and  $0.27 \mu\text{m}$  in height. TEM showed a similar fine particle structure down to  $50 \text{ nm}$  diameter. At platinum loadings in the range  $1\text{--}5 \text{ mg Pt cm}^{-2}$ , comparable  $R_f$  values and platinum surface areas were obtained to those achieved by magnetic stirring of the electrolytes (Table 1). Significantly, however, EPMA indicated that at a given platinum loading there was an increased degree of platinum penetration of the

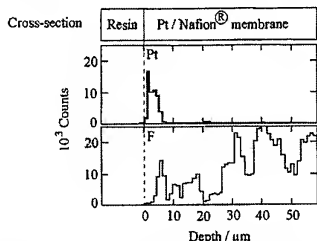


Fig. 6 EPMA traces across a Pt-coated Nafion 117 membrane prepared from  $0.02 \text{ mol dm}^{-3} \text{ H}_2\text{PtCl}_6$  and  $0.1 \text{ mol dm}^{-3} \text{ NaBH}_4$  in  $1 \text{ mol dm}^{-3} \text{ NaOH}$  with the cell mechanically shaken during a deposition time of 3 h.  $T = 295 \text{ K}$ ; the membrane surface was not roughened prior to platinum deposition. The vertical axis (distance = zero) corresponds to the surface of the membrane originally in contact with the  $\text{H}_2\text{PtCl}_6$  solution. Pt (top, thick line) and F (bottom, thin line) spectra have been peak-background corrected.

Table 1 Effect of solution agitation on platinum loading and surface area. Deposition conditions:  $0.02 \text{ mol dm}^{-3} \text{ H}_2\text{PtCl}_6$ ,  $0.1 \text{ mol dm}^{-3} \text{ NaBH}_4$  in  $1 \text{ mol dm}^{-3} \text{ NaOH}$ ; 3 h deposition time;  $T = 295 \text{ K}$ ; Nafion 117 membrane surface not roughened

Type of agitation	Pt loading, $\text{W/mg Pt cm}^{-2}$	Roughness factor, $R_f/\text{cm}^2 \text{ Pt cm}^{-2}$	Specific surface area, $\text{S/m}^2 \text{ g}^{-1} \text{ Pt}$
Manual shaking	3.9	278	7.1
Magnetic stirrer	4.1	686	16.7
Mechanical shaker	5.5	568	10.3
Flow-through cell	3.8	640	16.8

Table 2 Effect of surface roughening of Nafion 117 on the platinum surface area. The values in parentheses are for roughened membranes. Deposition conditions:  $0.1 \text{ mol dm}^{-3} \text{ NaBH}_4$  in  $1 \text{ mol dm}^{-3} \text{ NaOH}$ ; 3 h deposition time;  $T = 295 \text{ K}$ ; manual shaking employed; Nafion 117 surface pre-roughened with wet 1200 grade silicon carbide paper

$[\text{H}_2\text{PtCl}_6]/\text{mol dm}^{-3}$	Pt-loading, $\text{W/mg Pt cm}^{-2}$	Roughness factor, $R_f/\text{cm}^2 \text{ Pt cm}^{-2}$	Specific surface area, $\text{S/m}^2 \text{ g}^{-1} \text{ Pt}$
0.02	3.8 (3.9)	278 (997)	7.3 (25.6)
0.04	6.7 (7.1)	895 (2014)	13.4 (28.4)

membrane (up to 5–30  $\mu\text{m}$  at high  $\text{H}_2\text{PtCl}_6$  concentrations). This produced good adhesion. Most importantly, reproducibility of the platinum deposits was significantly improved over all other forms of solution agitation examined. This is a result of the well defined flow conditions in the cell.<sup>24</sup> It is important to have reproducible flow conditions to produce consistent platinum deposits of high specific surface area with good adhesion.

#### Effect of surface roughening of the Nafion 117 membrane

In an attempt to improve the roughness factor, specific surface area and adhesion of the platinum deposit, the surface of the Nafion 117 membrane was roughened with silicon carbide paper. Table 2 shows the effect of surface abrasion on the  $R_F$  value and platinum surface area at two concentrations of  $\text{H}_2\text{PtCl}_6$  and a fixed concentration of  $\text{NaBH}_4$ , with manual shaking of the cell. Surface abrasion resulted in an increase in the  $R_F$  value and specific platinum surface area by a factor of 2.3–3.5 at a selected platinum loading. This suggests that there was an increase in the number of platinum nucleation sites on the roughened membrane surface, leading to a much reduced platinum particle size. SEM, AFM and TEM analysis confirmed a reduction in the average diameter of the deposited platinum particles to well below the previously observed 100 nm. The topography of the platinum deposit was, however, little changed with the fine microstructure and micro- and macro-nodules on islands formed by cracks observed. EPMA analysis did show a second effect from membrane roughening. More of the platinum deposit was located within the membrane at a given platinum loading. This improved the adhesion of the deposit.

Combining the benefits of the surface roughening of Nafion 117 with those achieved by using the flow-through cell produced the highest quality Pt/Nafion structures achieved in this study. Reproducible platinum deposits with good adhesion, but with higher specific platinum surface areas (30–50  $\text{m}^2 \text{g}^{-1}$  Pt) were achieved over a range of platinum loadings. These deposits are much improved over previously reported studies<sup>17,18</sup> of platinum deposition on Nafion 117.

#### Comparison with conventional electrode technology

It is worth comparing the roughness factors and specific surface areas with those typically achieved using traditional gas diffusion electrode (GDE) technology employed in a number of applications, most notably proton exchange membrane fuel cells.<sup>25,26</sup> Such systems employ carbon supported platinum catalysts impregnated with Nafion membrane electrolyte solution to contact the metal in the electrodes. The GDEs are subsequently hot-pressed to the SPE membrane in applications where this is desired. By using high surface area carbon supports, platinum particle diameters of 2–5 nm are typically found, even after prolonged use.<sup>27</sup> This produces specific surface areas of 60–100  $\text{m}^2 \text{g}^{-1}$  Pt at platinum loadings of 40–20% m/m on the carbon support. This translates to  $R_F$  values in the range 3000–5000  $\text{cm}^2 \text{Pt cm}^{-2}$  at a GDE loading of 5 mg Pt  $\text{cm}^{-2}$  and 300–500  $\text{cm}^2 \text{Pt cm}^{-2}$  at a more economical GDE loading of 0.5 mg Pt  $\text{cm}^{-2}$ . At best, the use of roughened Nafion 117 surfaces in a flow-through cell produced a specific surface area of 30–50  $\text{m}^2 \text{g}^{-1}$  Pt. This translates to an  $R_F$  value of 1500–2500  $\text{cm}^2 \text{Pt cm}^{-2}$  at an electrode loading of 5 mg Pt  $\text{cm}^{-2}$  and to 250  $\text{cm}^2 \text{Pt cm}^{-2}$  at 0.5 mg Pt  $\text{cm}^{-2}$ . The potentially available platinum surface area is approximately 50% lower in the platinum-coated membrane electrodes. Although higher electrocatalyst surface areas do not necessarily translate to a higher performance as a result of kinetic, ohmic

and mass transport losses within the electrode matrix,<sup>27</sup> they do imply a potential benefit.

#### Conclusions

The preparation conditions influencing the properties of platinum-coated Nafion 117 materials for electrochemical applications were investigated using the procedure of Takenaka and co-workers<sup>17,18</sup> for the chemical deposition of platinum on to the membrane via  $\text{NaBH}_4$  reduction of  $\text{H}_2\text{PtCl}_6$ . Particular attention was given to  $\text{H}_2\text{PtCl}_6$  concentration, the electrolyte agitation conditions during the chemical deposition and to surface roughening of the Nafion 117 membrane as a pre-treatment.

The practical considerations for an 'ideal' structure include production of a porous deposit, a high surface area of platinum in contact with the Nafion membrane for good electrocatalysis and metal adhesion, with the platinum layer extending outside the membrane so that a current collector can be readily contacted.<sup>2</sup> To achieve this using the  $\text{NaBH}_4$  reduction of  $\text{H}_2\text{PtCl}_6$ , a high concentration of  $\text{H}_2\text{PtCl}_6$  should be used, with control of the electrolyte flow conditions and roughening of the Nafion membrane surface. Stirred or mechanically shaken conditions can be used but a flow-through cell using the plane, parallel plate geometry provides a preferred, controlled mass transport regime. The flow-through cell gives rise to a uniform deposit morphology and a controlled and high penetration beneath the Nafion 117 surface. In addition, a high platinum surface area was produced, principally owing to the efficient removal of hydrogen gas bubbles from the membrane surface. Roughening the membrane also raised the platinum surface area by increasing the number of nucleation sites available for platinum deposition. The combination of conditions used produced coherent platinum deposits with platinum surface areas at best around 50% of those achieved using current GDEs with carbon-supported catalysts. Further investigation of membrane pre-treatments and deposition conditions could give rise to improved platinum deposits.

#### Acknowledgements

Studentship support from the EPSRC (to S.-A.S.) is gratefully acknowledged. Mr. Mike Matthews (JMTC) provided valuable assistance with the EPMA and electron microscopy measurements.

#### Appendix

##### Symbols

$A_{\text{ec}}$	Electrochemical surface area	$\text{cm}^2 \text{Pt}$
$A_g$	Geometric surface area	$\text{cm}^2$
$A_r$	Real surface area	$\text{cm}^2 \text{Pt}$
$d$	Diameter of spherical particles	$\text{cm}$
$Q_m$	Electrical charge associated with monolayer adsorption of hydrogen	$210 \mu\text{C cm}^{-2} \text{Pt}$
$Q_h$	Charge associated with saturated hydrogen coverage	$\mu\text{C}$
$R_F$	Roughness factor	$\text{cm}^2 \text{Pt cm}^{-2}$
$S$	Specific surface area	$\text{cm}^2 \text{g}^{-1} \text{Pt}$
$T$	Temperature	$\text{K}$
$W$	Platinum-loading	$\text{g Pt cm}^{-2}$
$v$	Mean linear flow velocity of electrolyte	$\text{cm s}^{-1}$
$\rho$	Bulk density of platinum	$21.4 \text{ g cm}^{-3}$

## References

- 1 M. Wakizoo, O. V. Velev and S. Srinivasan, *Electrochim. Acta.*, 1995, **40**, 335.
- 2 P. S. Fedkiw, J. M. Potente and W.-H. Her, *J. Electrochem. Soc.*, 1990, **137**(5), 1451.
- 3 T. W. Kaaret and D. H. Evans, *Anal. Chem.*, 1988, **60**, 657.
- 4 T. A. Davis, J. D. Genders and D. Fletcher, *A First Course in Ion Permeable Membranes*, Electrochemical Consultancy, Romsey, 1997.
- 5 R. S. Yeo and H. L. Yeager, *Modern Aspects Electrochem.*, 1985, **16**, 437.
- 6 T. D. Gierke, G. B. Munn and F. C. Wilson, *J. Polym. Sci., Part B: Polym. Phys.*, 1981, **19**, 1687.
- 7 T. D. Gierke and W. Y. Hsu, in *Perfluorinated Ionomer Membranes*, ed. H. L. Yeager and A. Eisenberg, ACS Symposium Series, No. 180, American Chemical Society, Washington, DC, 1982, pp. 283–307.
- 8 B. Dreyfus, G. Gebel, P. Aldebert and M. Pineri, *J. Phys. (Paris)*, 1990, **51**, 1341.
- 9 P. C. Lee and D. Meisel, *J. Am. Chem. Soc.*, 1980, **102**, 5477.
- 10 T. Xun, J. S. Trent and K. Osseo-Asare, *J. Membr. Sci.*, 1989, **45**, 261.
- 11 H. L. Yeager and A. Eisenberg, in *Perfluorinated Ionomer Membranes*, ed. H. L. Yeager and A. Eisenberg, ACS Symposium Series, No. 180, American Chemical Society, Washington, DC, 1982, p. 1.
- 12 F. Delime, J. M. Leger and C. Lamy, *J. Appl. Electrochem.*, 1998, **28**, 27.
- 13 P. Millet, R. Durand and M. Pineri, *Int. J. Hydrogen Energy*, 1990, **15**(4), 245.
- 14 R. J. Lawrence and L. D. Wood, *US Pat.*, 4 272 353, 1981.
- 15 R. Banzinger, H.-J. Christen and S. Stucki, *US Pat.*, 4 396 469, 1983.
- 16 H. Nagel, *US Pat.*, 4 326 930, 1982.
- 17 H. Takenaka and E. Torikai, *Kokai Tokyo Koho (Jpn. Pat.)*, 55 38934, 1980.
- 18 H. Takenaka, E. Torikai, Y. Kawami and N. Wakabayashi, *Int. J. Hydrogen Energy*, 1982, **7**(5), 397.
- 19 R. Woods, *J. Electroanal. Chem.*, 1981, **9**, 9.
- 20 G. Binnig, C. F. Quate and C. Garber, *Phys. Rev. Lett.*, 1986, **59**, 930.
- 21 M. Andrae, K. Rohrbacher, P. Klein, L. Udvardy and J. Wernisch, *Scanning*, 1997, **19**(7), 477.
- 22 S. Kamasaki, S. Sekido, S. and Y. Miya, *Mem. Fac. Technol. Metropolitan Univ.*, 1988, **38**, 141.
- 23 L. E. Marling and S. Mazur, *J. Phys. Chem.*, 1986, **90**, 3269.
- 24 D. W. DeWulf and A. J. Bard, *J. Electrochem. Soc.*, 1988, **135**(8), 1977.
- 25 E. A. Ticianelli, C. R. Derouin and S. Srinivasan, *J. Electroanal. Chem.*, 1988, **251**, 275.
- 26 M. S. Wilson and S. Gottesfeld, *J. Electrochem. Soc.*, 1992, **139**(2), L28.
- 27 T. R. Ralph, G. A. Hards, J. E. Keating, S. A. Campbell, D. P. Wilkinson, M. Davis, J. St.-Pierre, and M. C. Johnson, *J. Electrochem. Soc.*, 1997, **144**(11), 3845.

Paper 8/03310B